J Mater Sci: Mater Med (2010) 21:907–914
DOI 10.1007/s10856-009-3911-1

Preparation and characterization of porous alginate scaffolds containing various amounts of octacalcium phosphate (OCP) crystals

Naru Shiraishi · Takahisa Anada · Yoshitomo Honda · Taisuke Masuda · Keiichi Sasaki · Osamu Suzuki

Received: 23 June 2009 / Accepted: 9 October 2009 / Published online: 23 October 2009

Abstract The present study was designed to investigate whether the amount of octacalcium phosphate (OCP) affects the characteristics of alginate (Alg)/OCP scaffolds regarding the pore formation and its distribution, and the thermodynamic stability from OCP to hydroxyapatite (HA) in an in vitro physiological environment. Alg/OCP composites with weight ratios of 100/0, 75/25, 50/50, and 25/75 were prepared through mixing the ground synthesized OCP crystals with an Alg solution and applying lyophilization. Analysis of X-ray diffraction, Fourier transform infrared (FTIR) spectroscopy, and mercury intrusion porosimetry verified that the crystalline phase of OCP and the porosities were retained regardless of the OCP amount. On the other hand, the elastic modulus, determined by mechanical testing, and, interestingly, the pore size increased with increasing the OCP amount. The immersion of the composites in a simulated body fluid up to 14 days revealed that OCP in Alg matrices tends to convert to HA with enhancing the calcium consumption depending on the OCP amount. The results indicated that the inclusion of OCP crystals in the Alg matrix by the mixing process controls the character of the pore distribution in Alg/OCP composites while maintaining the transitory nature of OCP.

N. Shiraishi · K. Sasaki
Division of Advanced Prosthetic Dentistry, Tohoku University Graduate School of Dentistry, 4-1 Seiryo-machi, Aoba-ku, Sendai 980-8575, Japan

N. Shiraishi · T. Anada · Y. Honda · T. Masuda · O. Suzuki (✉)
Division of Craniofacial Function Engineering (CFE), Tohoku University Graduate School of Dentistry, 4-1 Seiryo-machi, Aoba-ku, Sendai 980-8575, Japan
e-mail: suzuki-o@m.tains.tohoku.ac.jp

1 Introduction

Octacalcium phosphate ($Ca_8H_2(PO_4)_6 \bullet 5H_2O$; OCP) is a calcium phosphate compound with a Ca/P molar ratio of 1.33 and a triclinic crystal system [1]. OCP is known to be closely associated with hydroxyapatite ($Ca_{10}(PO_4)_6(OH)_2$; HA); the crystal structure of OCP is composed of apatite layers stacked with alternatively hydrated layers [1]. Based on the crystalline characteristics of OCP, this salt has been proposed as a precursor of apatite crystals in bone and tooth [2], although the existence of OCP in bone mineralization remains controversial [3, 4]. The osteoconductivity of synthetic OCP was first identified in its granule implantation in the subperiosteal region of mouse calvaria [5, 6]. Recently, the osteoconductive and biodegradable characteristics of OCP have been extensively recognized for various uses, such as coating forms, both in vitro and in vivo [7–10].

Our recent study reported that OCP improves a non-cell interactive polymeric scaffold alginate (Alg) to an osteogenic condition if precipitated directly on its three-dimensional (3D) porous sponge skeleton from calcium and phosphate solutions [11]. This previous study showed that (1) osteoblastic cell attachment in vitro increased with increasing the pore diameter from approximately 6–52 μm; (2) bone regeneration is enhanced the most in Alg/OCP with the largest pores (52 μm) in mouse critical-sized defects [11]. The results suggest that the pore character in the Alg/OCP scaffold critically controls the osteogenic condition in such OCP-distributed 3D scaffold [11],

as similarly reported in sintered bodies, such as HA ceramics [12]. In the preparation of Alg/OCP through direct precipitation, it seemed likely that Alg molecules regulate OCP precipitation kinetics caused by the interaction between the Alg molecules and the crystal surfaces [13, 14], resulting in the formation of pores up to 52 μm in diameter and the inhibition of the crystallization of OCP depending on the amount of OCP used.

It has been suggested that the mechanism to enhance bone formation by OCP is due to the transitory nature of OCP into HA in a physiological milieu [5, 6, 15, 16]. Bone formation has been confirmed to be facilitated during in situ OCP-HA conversion of the implanted OCP crystals [5, 6, 16]. Another study reported that mouse stromal osteoblastic cell differentiation increases dose-dependently with the application of OCP [17]. Thus, the enhancement of the conversion from OCP to HA and the amount of OCP included in an Alg scaffold may be factors to enhance the usefulness of this scaffold for bone regeneration.

The present study was designed to investigate whether the amount of OCP affects the material characteristics, including the pore size and the mechanical property, if Alg/OCP composites are prepared through mixing an Alg solution with pre-obtained well-grown OCP crystals. The conversion of OCP in the composites was examined by their immersion in a simulated body fluid as a conversion-accelerating test; this is because the conversion into HA is a very slow process [18] unless OCP is incubated in a supersaturated condition with respect to HA or in a promoter-included condition to form HA, such as fluoride [19], which raises the degree of supersaturation with respect to fluoridated HA [15].

2 Materials and methods

2.1 Material preparation

OCP was prepared according to a method reported previously [5]. Sodium alginate (MW = 64,000) was purchased from Wako Pure Chemical Industries (Osaka, Japan). Sodium alginate was dissolved in Milli-Q water to a concentration of 4% (w/v) and filtered through 1.2 μm nylon membrane filters. The synthetic OCP was ground using a pestle and a mortar. Then, the ground OCP powder (particle size under 100 μm) was mixed with the Alg solution and homogenized by a Multi-Beads Shocker (MB755U(S), Yasui-kikai, Osaka, Japan) at 2,800 rpm. This procedure reduced the size of OCP particles under 10 μm while keeping the plate-like crystal morphology (approximately 2–5 μm in length) intact. A calcium chloride solution was added to obtain the cross-link by the Ca^{2+} ions. Alg/OCP slurries containing different amounts of OCP (w/w% = 100/0, 75/25, 50/50, and 25/75) were prepared. These mixtures were referred to as Alg/OCP (100/0), Alg/OCP (75/25), Alg/OCP (50/50), and Alg/OCP (25/75). Three percent (w/v) sodium alginate and 50 mM calcium chloride were used to prepare the slurry with OCP. The slurries were centrifuged at 15,000 rpm for 5 min in order to exclude the supernatant containing the redundant Ca^{2+} ions, and deposits were then re-suspended in water. Re-suspended slurries were placed in a plastic tube (9 mm diameter), frozen in the −30°C, and then lyophilized to form porous scaffolds.

2.2 Characterization of OCP crystals and Alg/OCP composites

The Alg/OCP composites were characterized by X-ray diffraction (XRD). The powder XRD pattern of the composites was recorded using step scanning at 0.2° intervals from 3.5–40°, with Cu Kα X-rays on a diffractometer (MiniFlex; Rigaku Electrical, Tokyo, Japan) at 30 kV and 15 mA. The XRD patterns thus obtained were compared with JCPDS numbers 26-1056A9 for OCP to identify the crystalline phases. The Fourier transform infrared (FTIR) spectrum of the composites was obtained by FTIR spectroscopy (FT/IR-6300, JASCO, Tokyo, Japan), with the sample diluted with potassium bromide, over the range of 2,000–400 cm^{-1} with 4 cm^{-1} resolution. The surface morphologies of the prepared composite sections were observed using scanning electron microscopy (SEM: JSM-6390LA, JEOL, Tokyo, Japan). The porosity and pore size were quantified by mercury intrusion porosimetry (Auto Pore IV 9510, Micromeritics Instrument Corp., Atlanta, GA, USA).

2.3 Mechanical testing

The uniaxial compressive test of the scaffolds was carried out on column blocks of approximately 5 mm in diameter. The tests were carried out on a universal testing machine (EZ-L-500N, SHIMADZU Co., Kyoto, Japan) in air at a constant crosshead speed of 0.5 mm/min, and the stress–strain curve was recorded by computer. The elastic moduli of the scaffolds were calculated as the slope of the initial linear portion of this stress–strain curve.

2.4 Immersion in simulated body fluid (SBF)

SBF was prepared according to a previous method [20] by dissolving a reagent grade of each sodium chloride, sodium hydrogen carbonate, potassium chloride, dipotassium hydrogen phosphate trihydrate, magnesium chloride hexahydrate, and calcium chloride dihydrate in purified water. The solution was then adjusted as pH 7.4 with

trihydroxymethyl aminomethane and hydrochloric acid to obtain pH at 37°C ($[Na^+] = 142.0$ mM, $[K^+] = 5.0$ mM, $[Mg^{2+}] = 1.5$ mM, $[Ca^{2+}] = 2.5$ mM, $[Cl^-] = 148.8$ mM, $[HCO^{3-}] = 4.2$ mM, $[HPO_4^{2-}] = 1.0$ mM, $[SO_4^{2-}] = 0.5$ mM). Four mg of Alg/OCP was immersed in 20 ml of the fresh SBF in separate plastic tubes and kept at 37°C for up to 14 days. The immersed composites were collected at 7 and 14 days. Those materials were lyophilized for FTIR spectroscopy and SEM observation. The concentration of calcium (Ca^{2+}) ions in the SBF was determined quantitatively by Ca–E test Wako (Wako Pure Chemical Industries, Osaka, Japan). After soaking for 14 days, the supernatants were collected for Ca^{2+} quantitative analyses.

2.5 Statistical analysis

Results were expressed as the mean ± standard deviation (SD). All experiments were performed with at least three individual replicates and showed reliable reproducibility. The Steel–Dwass test was used for comparing the results of mechanical testing. One-way analysis of variance (ANOVA) was used to compare the changes of Ca^{2+} concentration of the supernatant of SBF after the Alg/OCP composites were immersed in SBF. If the ANOVA was significant, the Dunnet test was used as a post hoc test.

3 Results and discussion

3.1 Characterization of Alg/OCP composites

Synthetic OCP cannot be molded by sintering processes because of the intrinsic crystal structure of OCP, which includes a large number of water molecules within the layered structure [1]. The combination of OCP (Fig. 1E) with Alg overcomes the poor moldability. Prepared Alg/OCP composites can be molded into various shapes, such as rod-shaped scaffolds, as shown in Fig. 1A–D.

Figure 2A shows the XRD patterns of Alg/OCP (100/0) (a), Alg/OCP (75/25) (b), Alg/OCP (50/50) (c), Alg/OCP (25/75) (d), and the original OCP (e). The XRD patterns obtained in the control OCP (e) and the Alg/OCP composites (b–d) contained the characteristic reflections (100) at $2\theta = 4.8°$ and (700) at $2\theta = 33.6°$. These features corresponded well to those expected from the OCP structure [21]. No specific peaks were observed in pure alginate (Alg/OCP (100/0)), indicating an amorphous-like structure. The characteristics of the crystal structure of OCP tended to be unclear with increasing Alg concentration in the composite. Figure 2B shows the FTIR spectra of Alg/OCP (100/0) (a), Alg/OCP (75/25) (b), Alg/OCP (50/50) (c), Alg/OCP (25/75) (d), and the original OCP (e). Three distinct bands originating from v_3 P–O in the orthophosphate stretch absorption around 1030–1130 cm^{-1} and HPO_4^{2-} bands at 906 and 852 cm^{-1} typical of the OCP structure were observed in the spectra of the original OCP (e) and the Alg/OCP composites (b–d). Two sharp absorption bands of v_4 PO_4 at 560–600 cm^{-1} were ascribed to crystalline calcium phosphate [22]. The 1,620 and 1,416 cm^{-1} bands are assigned to the antisymmetric and symmetric COO^- stretching vibration of the salified carboxyl group of alginic acid, respectively. The intensity of these bands assigned to alginate decreased with increasing the OCP ratio in the composites. The v_3 PO_4 region (900–1200 cm^{-1}) of the OCP structure became broader in the spectra of the Alg/OCP composites. In both XRD and FTIR results, the characteristic peaks of OCP were maintained in the composites, suggesting that the alginate did not induce subsequent modifications in the crystal structure of OCP. Moreover, the spectral changes of the XRD and FTIR obtained in Alg/OCP composites suggest the formation of inorganic–organic hybrid scaffolds [13, 14].

Figure 3 shows SEM micrographs of Alg/OCP (100/0) (A, B), Alg/OCP (75/25) (C, D), Alg/OCP (50/50) (E, F), and Alg/OCP (25/75) (G, H). Alg/OCP (100/0) was highly porous and had a well-interconnected pore structure

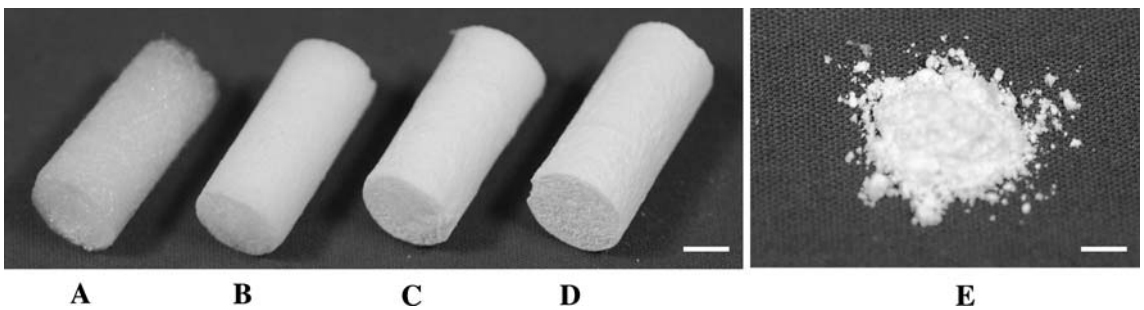

Fig. 1 Photographs of **A** Alg/OCP (100/0), **B** Alg/OCP (75/25), **C** Alg/OCP (50/50), **D** Alg/OCP (25/75), and **E** original OCP granules. Bars = 5 mm

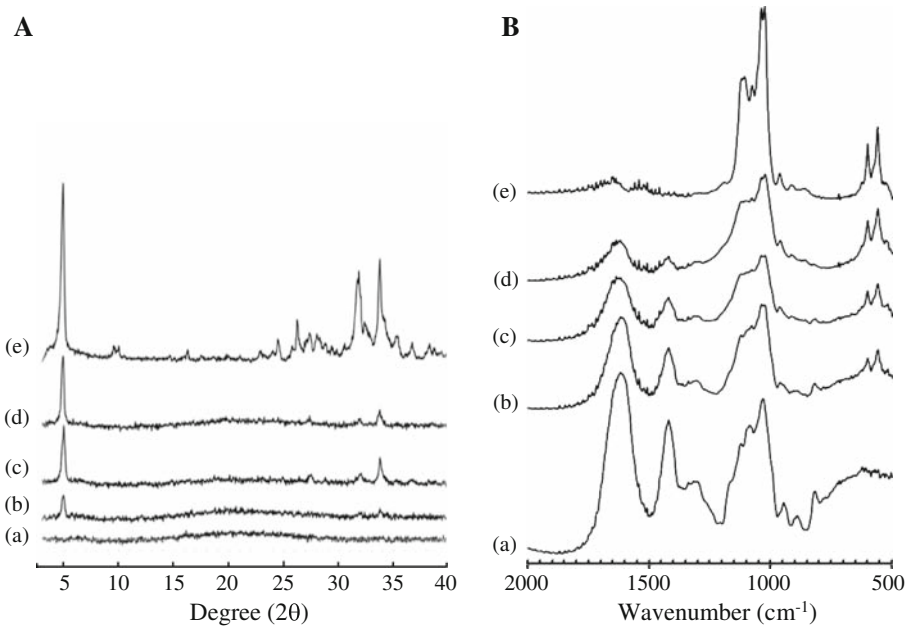

Fig. 2 XRD patterns **A** of (*a*) Alg/OCP (100/0), (*b*) Alg/OCP (75/25), (*c*) Alg/OCP (50/50), (*d*) Alg/OCP (25/75), and (*e*) original OCP and FTIR spectra **B** of (*a*) Alg/OCP (100/0), (*b*) Alg/OCP (75/25), (*c*) Alg/OCP (50/50), (*d*) Alg/OCP (25/75), and (*e*) original OCP

(Fig. 3A). In higher magnification, Alg/OCP (100/0) exhibited smooth surfaces with a sheet-like morphology (Fig. 3B). A highly porous, well-interconnected pore structure was also observed in the Alg/OCP composites (Fig. 3C, E, G), although the pore size of the composites was clearly different from that of Alg/OCP (100/0). In the Alg/OCP (75/25) composite, OCP crystals were partially embedded within the Alg matrix throughout the walls (Fig. 3D). On the other hand, in the Alg/OCP (50/50) and (25/75) composites, OCP crystals were observed as a plate-like morphology about 2–5 μm in length on the surface as well as the inner walls of the scaffolds (Fig. 3F, H). The surfaces of the Alg/OCP composites were rough, and OCP crystals were homogeneously dispersed in the polymer matrix.

The quantitative analysis of the pore size and porosity of the prepared composites, as determined by mercury intrusion porosimetry, is shown in Table 1. The size of relatively large pores (over 50 μm) tended to increase with increasing the amount of OCP, as seen in Fig. 3, while the porosity of each sample was almost identical (ranging from 80 to 85%). At present, although the precise mechanism leading to different pore sizes in the pure alginate and the composites is still unclear, a possible explanation is that the size of ice crystals formed in the freezing process may be different between the pure alginate and the composites due to the interaction of OCP crystals with water molecules, depending on the OCP amount. We previously reported that OCP-precipitated Alg scaffolds prepared by co-precipitation had approximately 52 μm pores [11]. On the other hand, the simple mixture of OCP powder and an alginate polymer solution presented in the present study yielded pores with an average size of 120 μm (Alg/OCP (50/50) and (25/75)). These results suggest that the preparation method by the simple mixing of OCP and alginate forms larger pores than accomplished with the co-precipitation method.

In the Alg/OCP (25/75) composite, ultrafine pores (~100 nm) were detected. We previously reported that the ultrafine pores were produced from voids between the OCP crystals [11, 23]. However, in the present Alg/OCP composites with ratios of 75/25 and 50/50, the ultrafine pores were not detected regardless of the inclusion of the OCP crystals in the Alg matrix, most probably due to the lower amount of OCP crystals relative to that of the Alg/OCP (25/75). It has been reported that the bimodal distribution of pores (i.e., ultrafine pores and micrometer-sized pores) was important for improved bone cell activity due to protein adsorption [24]. The porous scaffolds allow cells to migrate and tissues to grow inward into their constructs. It is anticipated that the larger pore size of the Alg/OCP scaffold may provide a site for the growth and migration of osteoblastic cells.

3.2 Mechanical property of Alg/OCP composites

Figure 4 shows the elastic modulus of the composites prepared with different OCP amounts. During the compression test, none of the Alg/OCP composites showed a final facture; however, they showed densification even when up to 75 wt% of the inorganic brittle OCP was added. The elastic modulus of the composites increased with the

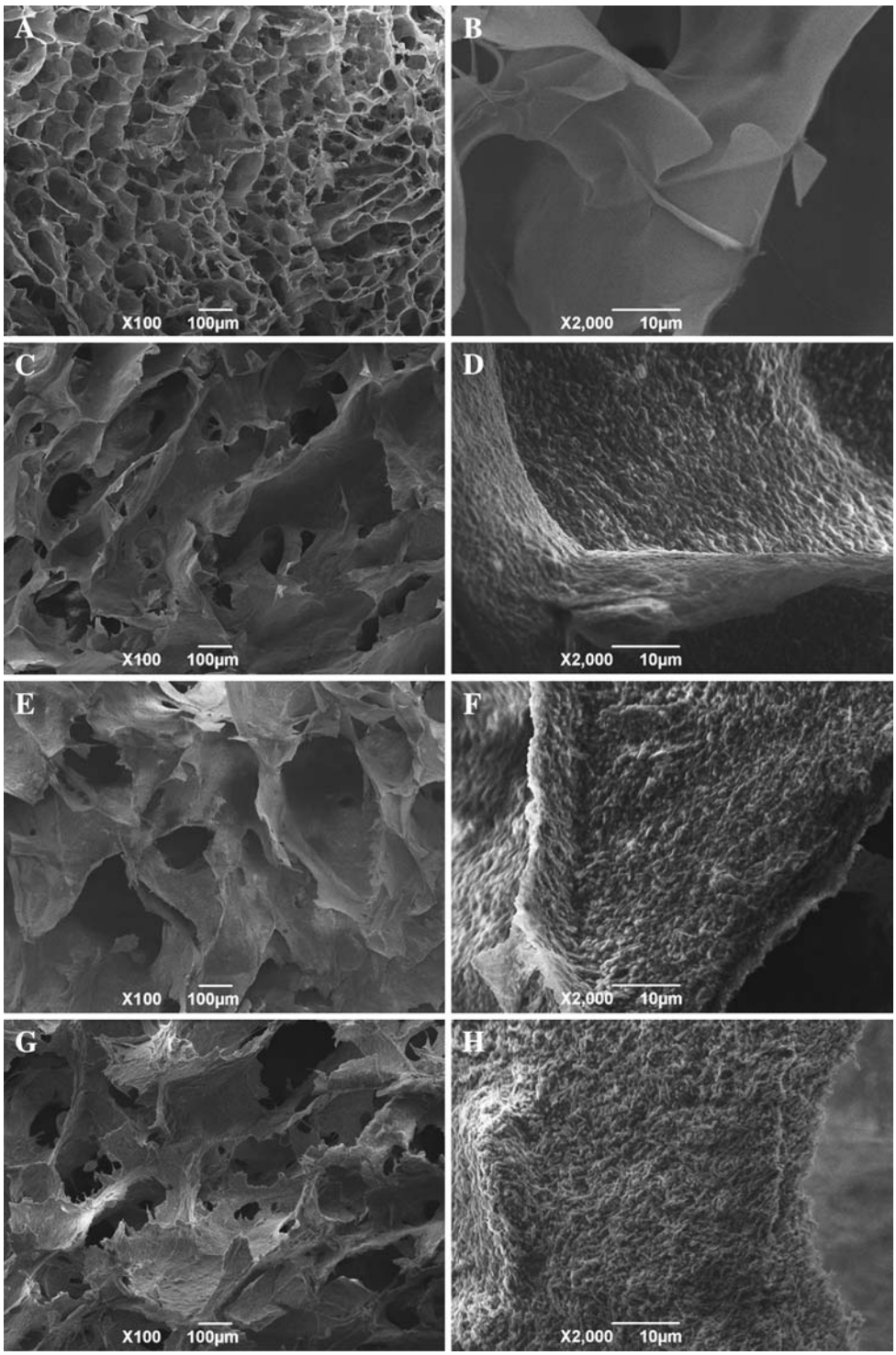

Fig. 3 SEM micrographs of Alg/OCP composites. **A**, **B** Alg/OCP (100/0); **C**, **D** Alg/OCP (75/25); **E**, **F** Alg/OCP (50/50); **G**, **H** Alg/OCP (25/75). Bars = 100 μm (**A**, **C**, **E**, **G**), 10 μm (**B**, **D**, **F**, **H**)

increase in the OCP amount. These results demonstrated that the mechanical properties of porous scaffolds were significantly affected by the amount of OCP in the composite. Despite the fact that the porosity of all the composites remained nearly constant and the pore size of Alg/OCP (50/50) and (25/75) composites was larger than that of other composites, the elastic modulus of the Alg/OCP (50/50) and (25/75) composites was higher than that of other composites. This may be due to an increase in the pore wall thickness and the density of these composites.

Table 1 Characterization of Alg/OCP composites prepared

Alg/OCP (%, weight/weight)	Pore size		Porosity (%)
	Large pores (μm)	Ultrafine pores (nm)	
100/0	51.8	n.d.	80.1
75/25	72.2	n.d.	84.2
50/50	119.8	n.d.	82.4
25/75	119.8	95.6	85.0

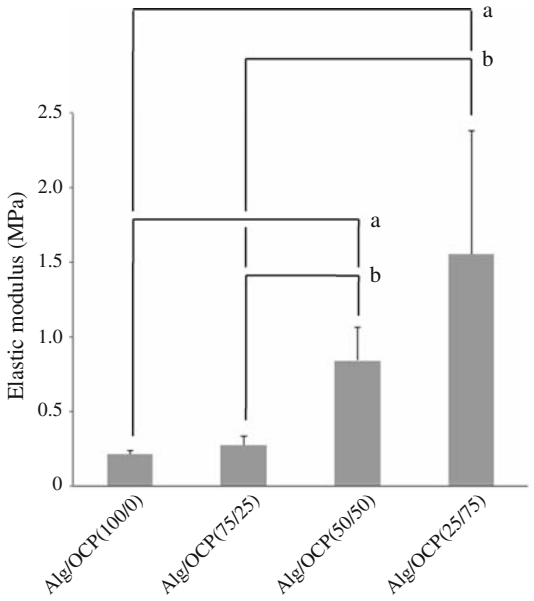

Fig. 4 Elastic modulus of Alg/OCP composites. Data are the mean ± SD ($n = 5$). [a] $P < 0.05$ compared with Alg/OCP (100/0). [b] $P < 0.05$ compared with Alg/OCP (75/25)

3.3 Conversion of OCP within Alg/OCP composites immersed in SBF

It has been reported that the osteoconductivity of biomaterials can be evaluated by examining the ability of apatite formation on their surfaces in SBF with ion concentrations nearly equal to those of human blood plasma [20]. On the contrary, the general method of testing remains controversial [25]. We previously reported that synthetic OCP tended to convert to HA in a Tris buffer at 37°C in the presence of fluoride ions [19], in a SBF solution [11], and in the living body [16], which suggests the importance of the transitory nature of OCP in a physiological environment. The conversion rate of OCP to HA highly depends on the crystallinity of OCP [26]. The conversion rate of well-grown OCP is very low [19]. Therefore, we used SBF as a conversion-accelerating agent by utilizing the degree of supersaturation.

Figure 5A shows the FTIR spectra of the Alg/OCP (75/25) composite, as a typical result, immersed in SBF for up to 14 days. The characteristic peaks of OCP at 1030–1130 cm^{-1} became obscured with time. As shown in the SEM images of Alg/OCP (75/25), before immersion in SBF, the crystals displayed an acicular morphology of short platy crystals, which was a morphological feature of OCP (Fig. 5B-a). The morphologies of the surface of the composites soaked in SBF for 14 days were obviously different from those of the original composites. Many granular crystals were deposited on the surface of the composites (Fig. 5B-b). The FTIR spectral changes and SEM images before and after the immersion in SBF could be caused by not only structural conversion from OCP to HA but also direct deposition and/or dissolution/re-precipitation of HA. Nearly identical results were obtained in the FTIR spectral changes and SEM observations of the other Alg/OCP composites (data not shown). Differently from the Alg/OCP composites, Alg/OCP (100/0) did not show any changes in FTIR spectra and SEM images before or after the immersion in SBF.

Figure 5C shows the results of chemical analyses of the supernatants of the composites after 14 days of incubation in SBF at 37°C. The Ca^{2+} concentration of the supernatant of the Alg/OCP composites decreased with increasing the amount of OCP in the composites. Previous studies showed that the OCP-apatite conversion induces the uptake of Ca^{2+} ions in physiological conditions [15, 17]. Therefore, the results support the concept that the OCP in the composites can convert to HA in SBF, although it has been reported that the presence of a high concentration of polyanions, such as polyacrylate, inhibits the hydrolysis of OCP to HA [27].

4 Conclusions

We have already reported on the fabrication of Alg/OCP composite scaffolds (OCP-precipitated Alg) by the co-precipitation method [11]. OCP-precipitated Alg with an average pore size of 52 μm showed the conversion of OCP to HA in SBF, better cell attachment and proliferation, and the enhancement of in vivo bone regeneration in mouse critical-sized calvaria bone defects. In the present study, we successfully developed novel Alg/OCP composite scaffolds fabricated by a simple mixing method. We found that the pore size of the composites was dependent on the OCP

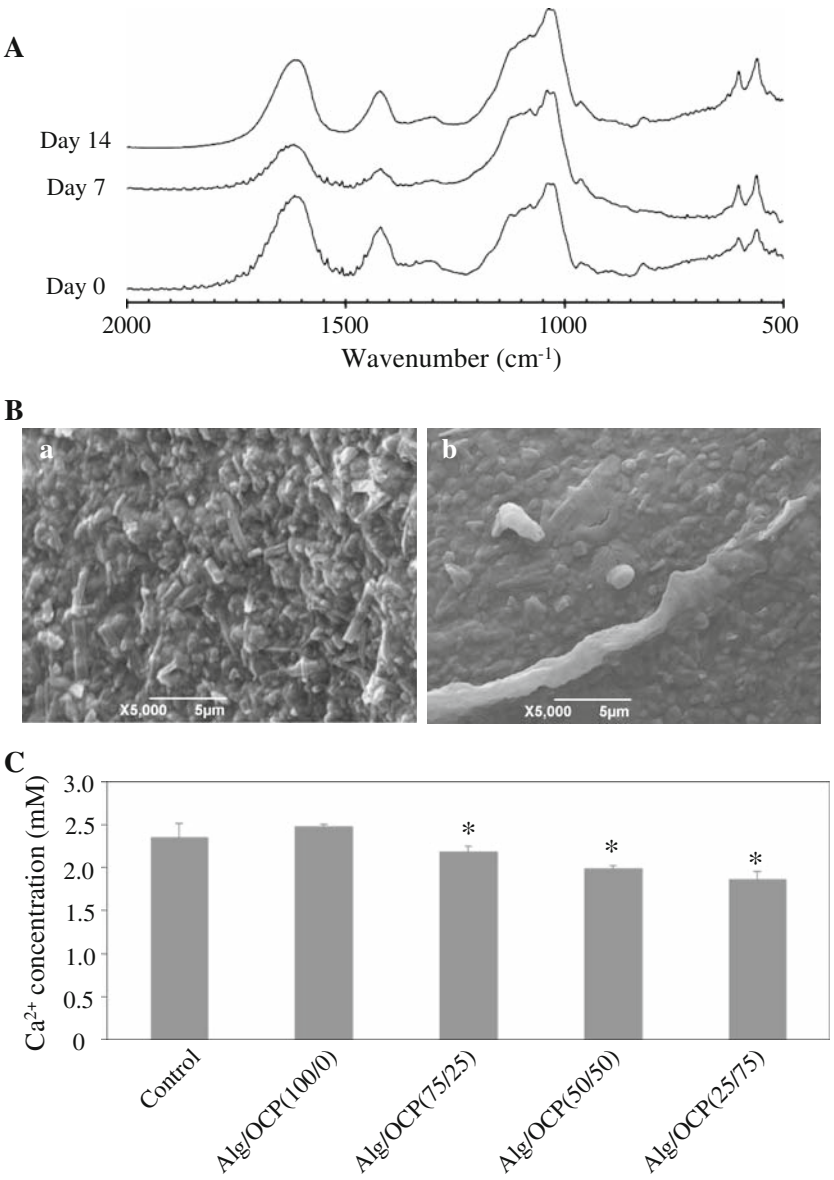

Fig. 5 FTIR spectra **A** of immersed Alg/OCP (75/25) in SBF for 0 (before immersion), 7, and 14 days. SEM images **B** for (*a*) 0 (before immersion) and (*b*) 14 days. Bars = 5 μm. Ca^{2+} concentrations **C** in SBF at 37°C after 14 days of immersion. Data are the mean ± SD ($n = 3$). * $P < 0.01$ compared with control

amount in the slurry. The Alg/OCP (50/50) and (25/75) composites had approximately 120 μm of pore diameter. It has been pointed out that a pore diameter of 100 μm is effective for bone ingrowth in porous implant materials [28]. Moreover, we previously reported that bone regeneration in rat critical-sized calvaria bone defects using a composite of OCP and collagen can significantly be promoted in an OCP dose-dependent manner in a collagen matrix [29]. These results suggest that Alg/OCP composites with a high concentration of OCP have the potential for providing a better scaffold for osteoblast proliferation and enhancement of bone regeneration.

Acknowledgments This study was supported in part by Grants-in-Aid (17076001, 19390490, 20659304) from the Ministry of Education, Science, Sports, and Culture of Japan.

References

1. Brown WE, Smith JP, Lehr JR, Frazier AW. Crystallographic and chemical relations between octacalcium phosphate and hydroxyapatite. Nature. 1962;196:1050–5.
2. Brown WE. Crystal growth of bone mineral. Clin Orthop Relat Res. 1966;44:205–20.
3. Grynpas MD, Omelon S. Transient precursor strategy or very small biological apatite crystals? Bone. 2007;41:162–4.
4. Weiner S. Transient precursor strategy in mineral formation of bone. Bone. 2006;39:431–3.
5. Suzuki O, Nakamura M, Miyasaka Y, Kagayama M, Sakurai M. Bone formation on synthetic precursors of hydroxyapatite. Tohoku J Exp Med. 1991;164:37–50.
6. Suzuki O, Nakamura M, Miyasaka Y, Kagayama M, Sakurai M. Maclura pomifera agglutinin-binding glycoconjugates on converted apatite from synthetic octacalcium phosphate implanted into subperiosteal region of mouse calvaria. Bone Miner. 1993;20:151–66.

7. Barrere F, van der Valk CM, Dalmeijer RA, Van Blitterswijk CA, de Groot K, Layrolle P. Photosensitized degradation of bisphenol A involving reactive oxygen species in the presence of humanic substances. J Biomed Mater Res A. 2003;64:378–86.
8. Bigi A, Bracci B, Cuisinier F, Elkaim R, Fini M, Mayer I, et al. Human osteoblast response to pulsed laser deposited calcium phosphate coatings. Biomaterials. 2005;26:2381–89.
9. Habibovic P, Van der Valk CM, Van Blitterswijk CA, De Groot K, Meijer G. Influence of octacalcium phosphate coating on osteoinductive properties of biomaterials . J Mater Sci Mater Med. 2004;15:373–80.
10. Shelton RM, Liu Y, Cooper PR, Gbureck U, German MJ, Barralet JE. Bone marrow cell gene expression and tissue construct assembly using octacalcium phosphate microscaffolds. Biomaterials. 2006;27:2874–81.
11. Fuji T, Anada T, Honda Y, Shiwaku Y, Koike H, Kamakura S, et al. Tissue Eng Part A. 2009; doi:10.1089/ten.tea.2009.0048.
12. Tamai N, Myoui A, Tomita T, Nakase T, Tanaka J, Ochi T, et al. Novel hydroxyapatite ceramics with an interconnective porous structure exhibit superior osteoconduction in vivo. J Biomed Mater Res. 2002;59:110–7.
13. Ribeiro CC, Barrias CC, Barbosa MA. Calcium phosphate-alginate microspheres as enzyme delivery matrices. Biomaterials. 2004;25:4363–73.
14. Zhao K, Cheng G, Huang J, Ying X. Reactive and functional polymers. React Funct Polym. 2008;68:732–41.
15. Suzuki O, Kamakura S, Katagiri T. Surface chemistry and biological responses to synthetic octacalcium phosphate. J Biomed Mater Res Appl Biomater. 2006;77B:201–12.
16. Suzuki O, Kamakura S, Katagiri T, Nakamura M, Zhao B, Honda Y, et al. Bone formation enhanced by implanted octacalcium phosphate involving conversion into Ca-deficient hydroxyapatite. Biomaterials. 2006;27:2671–81.
17. Anada T, Kumagai T, Honda Y, Masuda T, Kamijo R, Kamakura S, et al. Dose-dependent osteogenic effect of octacalcium phosphate on mouse bone marrow stromal cells. Tissue Eng Part A. 2008; 14:965–78.
18. Tung MS, Tomazic B, Brown WE. The effects of magnesium and fluoride on the hydrolysis of octacalcium phosphate. Arch Oral Biol. 1992;37:585–91.
19. Suzuki O, Yagishita H, Yamazaki M, Aoba T. Adsorption of bovine serum albumin onto octacalcium phosphate and its hydrolyzates. Cells Mater. 1995;5:45–54.
20. Kokubo T, Takadama H. How useful is SBF in predicting in vivo bone bioactivity?. Biomaterials. 2006;27:2907–15.
21. Mathew M, Brown W, Schroeder L, Dickens B. Crystal-structure of octacalcium bis(hydrogenphosphate) tetrakis(phosphate) pentahydrate, $Ca_8(HPO_4)_2(PO_4)_4{\cdot}5H_2O$. J Crys Spectrosc. 1988;18: 235–50.
22. Fowler BO, Moreno EC, Brown WE. Infra-red spectra of hydroxyapatite, octacalcium phosphate and pyrolysed octacalcium phosphate. Arch Oral Biol. 1966;11:477–92.
23. Kikawa T, Kashimoto O, Imaizumi H, Kokubun S, Suzuki O. Intramembranous bone tissue response to biodegradable octacalcium phosphate implant. Acta Biomater. 2009;5:1756–66.
24. Pek YS, Gao S, Arshad MA, Leck K-J, Ying J. Porous collagen-apatite nanocomposite foams as bone regeneration scaffolds. Biomaterials. 2008;29:4300–5.
25. Bohner M, Lemaitre J. Can bioactivity be tested in vitro with SBF solution? Biomaterials. 2009;30:2175–9.
26. Mura-Galelli MJ, Narusawa H, Shimada T, Iijima M, Aoba T. Effects of fluoride at low concentrations on precipitation of calcium phosphatesin media simulating the enamel fluid. Cells Mater. 1992;2:221–30.
27. Bigi A, Boanini E, Borghi M, Cojazzi G, Panzavolta S, Roveri N. Synthesis and hydrolysis of octacalcium phosphate: effect of sodium polyacrylate. J Inorg Biochem. 1999;75:145–51.
28. Jarcho M. Calcium phosphateceramics as hard tissue prosthetics. Clin Orthop. 1981;157:259–78.
29. Kawai T, Anada T, Honda Y, Kamakura S, Matsui K, Matsui A, et al. Synthetic octacalcium phosphate augments bone regeneration correlated with its content in collagen scaffold. Tissue Eng Part A. 2008;15:23–32.